

# Unique porous $\text{LiCoO}_2$ thin layers prepared by electrostatic spray deposition

C. H. CHEN\*, E. M. KELDER, J. SCHOONMAN

*Laboratory for Applied Inorganic Chemistry, Delft University of Technology, Julianalaan 136, 2628 BL Delft, The Netherlands*

Electrostatic spray deposition (ESD) technique was used to fabricate thin  $\text{LiCoO}_2$  layers on a metal substrate. A unique, highly porous structure with a narrow pore-size distribution around  $1\text{ }\mu\text{m}$  was obtained at  $230^\circ\text{C}$  using acetates as precursors and a mixture of ethanol (15 vol %) and butyl carbitol (85 vol %) as solvent. The pores were three-dimensionally interconnected. This structure was thermally stable at temperatures up to  $600^\circ\text{C}$ . At small flow rates of the precursor solution, a nearly linear relation was found between pore size and flow rate. At deposition temperatures above  $230^\circ\text{C}$  the porous structure disappeared. A possible formation mechanism for the porous structure has been proposed.

## 1. Introduction

During our exploration to apply the electrostatic spray pyrolysis (ESP) technique to the fabrication of thin films of solid electrolytes and lithium battery electrode materials [1–4], we recently discovered the formation of unique porous structures with certain metal oxides ( $\text{LiMn}_2\text{O}_4$ ,  $\text{SnO}_2\text{--MnO}_2$  and  $\text{LiCoO}_2$ ) [5]. The structures are highly porous and have a narrow pore-size distribution. The pores are three-dimensionally interconnected. The present layers or coatings are of interest for the fields of catalysis, chemical sensors, inorganic membranes, and electrode materials for solid oxide fuel cell (SOFC) and batteries due to their high assured surface area. This report focuses on  $\text{LiCoO}_2$  layers with such structure, with emphasis on the possible formation mechanism and the thermal stability of this structure. It is also shown that the pore size can be tailored from micrometre to sub-micrometre range.

## 2. Experimental procedure

An aerosol deposition technique was adopted in this study, the electrostatic spray deposition (ESD) technique, which was also called electrostatic spray pyrolysis (ESP) in our previous reports. Lithium acetate dihydrate ( $\text{Li}(\text{CH}_3\text{COO})\cdot 2\text{H}_2\text{O}$ ) and cobalt acetate tetrahydrate ( $\text{Co}(\text{CH}_3\text{COO})_2\cdot 4\text{H}_2\text{O}$ ) of analytical grade were used as precursors, and dissolved in a mixture of ethanol ( $\text{C}_2\text{H}_5\text{OH}$ , 15 vol %) and butyl carbitol ( $\text{CH}_3(\text{CH}_2)_3\text{OCH}_2\text{CH}_2\text{OCH}_2\text{CH}_2\text{OH}$ , 85 vol %). A 0.005 M solution was prepared.

The ESD set-up used in this study is of a vertical configuration with the substrate positioned right above the nozzle, as shown in Fig. 1. The set-up operates in a fume hood. The precursor solution was fed

into the nozzle by a rotatory pump (Watson Marlow 101U) which could control the flow rate from  $0.16\text{--}8\text{ ml h}^{-1}$ . The substrate temperature was controlled by the voltage applied to the heating element. Stainless steel discs (1 mm thick, 14 mm diameter) were used as substrate. However, some experiments were also performed with porous nickel plates. When a high voltage of 8–10 kV was applied between the nozzle (made from stainless steel) and the substrate, 2 cm apart, a fine spray was generated from the nozzle and a thin layer was deposited on the substrate. A Jeol JSM-35 model scanning electron microscope provided with an energy dispersive X-ray microanalyser (EDX) (Link ISIS, Oxford Instruments Ltd) was used in order to observe the morphology and to analyse the compositions of the deposited layers.

## 3. Results and discussion

Fig. 2 shows the surface morphologies of  $\text{LiCoO}_2$  layers deposited at  $230^\circ\text{C}$ . The films are highly porous with narrow pore-size distributions. The pores are three-dimensionally cross-linked. Only a small carbon peak was detected by EDX. After heat treatment at  $400^\circ\text{C}$  the weight loss accounts for about 10 % of its initial weight. This means that this porous structure mainly consists of oxides of lithium and cobalt. They appear to be crack-free, which shows an advantage of the deposition technique over normal wet-chemical processes such as the sol–gel deposition process.

In addition, it was also observed that the pore size changes with the feed rate (or flow rate) of the precursor solution, as shown in Fig. 3. At small flow rates, from (a) to (c) in Fig. 3, the average pore size was approximately proportional to the flow rate. However, the pore size–flow rate curve seems to level off at

\* Author to whom all correspondence should be addressed.

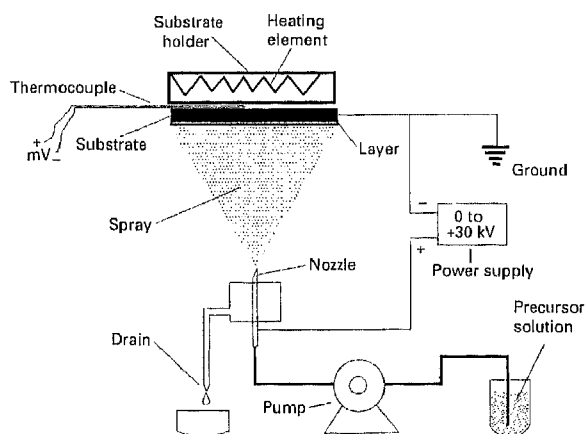


Figure 1 Schematic illustration of the vertical ESD set-up.

relatively large flow rates. This could be explained by the effect of the flow rate on the primary droplet size produced by the spray nozzle. According to the scaling law for polar liquids [6], the primary droplet size,  $d$ , is proportional to  $(Q/\kappa)^{1/3}$ , where  $Q$  and  $\kappa$  are the flow rate and electric conductivity of the precursor solution, respectively. Because the volume of the primary droplet  $V = \pi d^3/6$  and the solute mass in a primary droplet  $m = VCM$  (where  $C$  is molar concentration of the solution and  $M$  the molecular weight of the solute), both  $V$  and  $m$  become proportional to the flow rate  $Q$ , i.e.  $V \propto Q$  and  $m \propto Q$ . Owing to the fact that the boiling point of the solvent is fairly high (230 °C for butyl carbitol and 78 °C for ethanol) and the substrate temperature is relatively low (230 °C), it might be

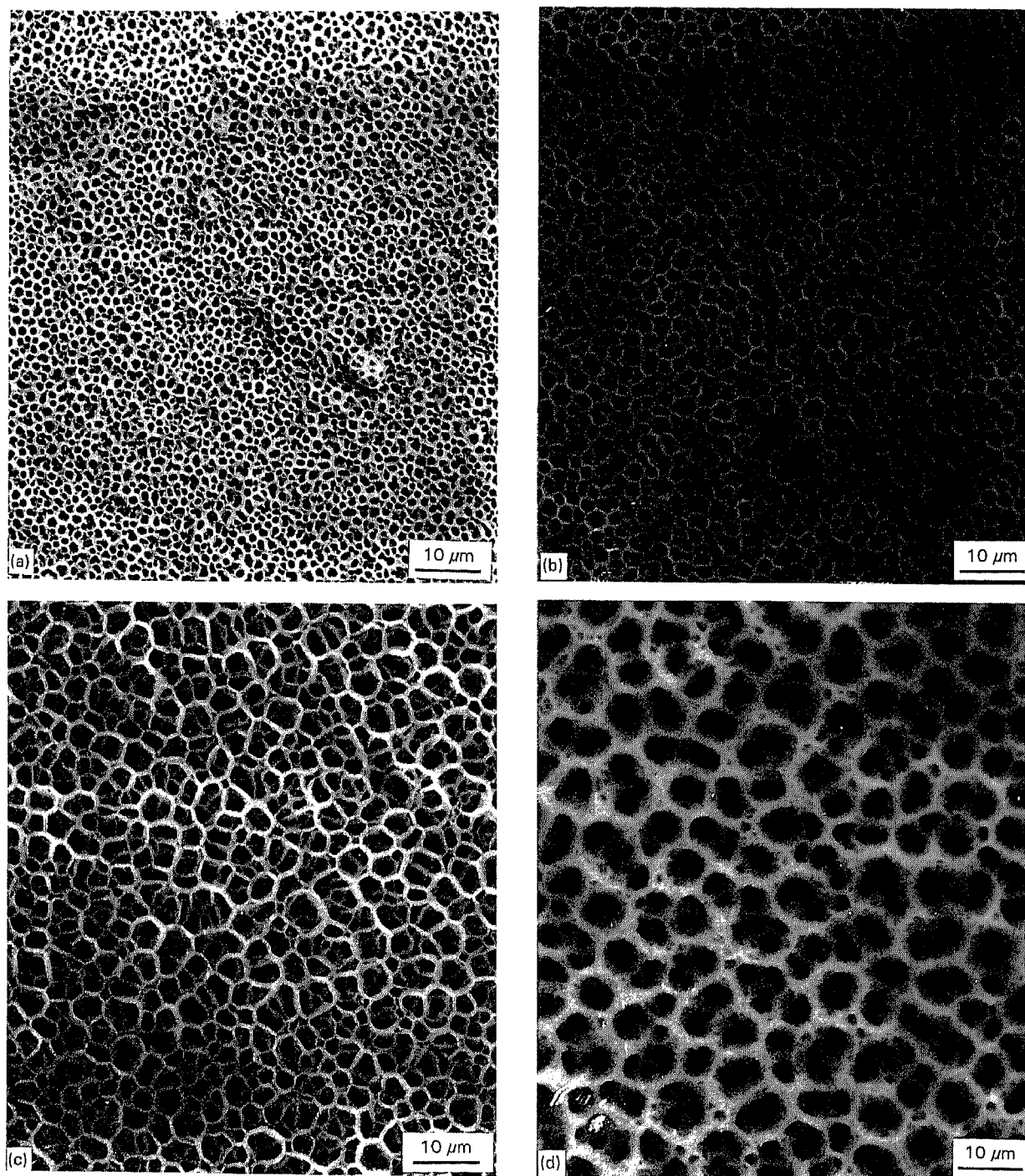


Figure 2 Scanning electron micrographs of  $\text{LiCoO}_2$  layers deposited on stainless steel at 230 °C for about 2 h with different flow rates: (a) 0.162  $\text{ml h}^{-1}$ ; (b) 0.404  $\text{ml h}^{-1}$ ; (c) 0.808  $\text{ml h}^{-1}$ ; (d) 1.616  $\text{ml h}^{-1}$ ; (e) 2.424  $\text{ml h}^{-1}$ .

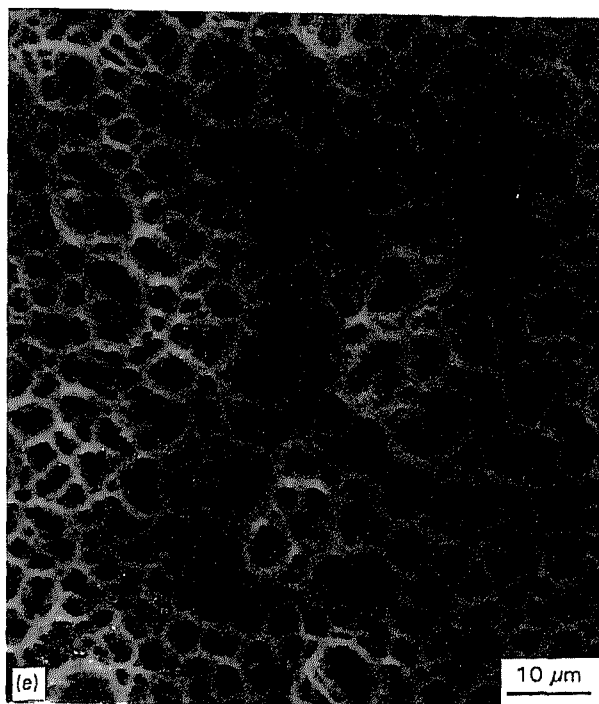


Figure 2 Continued.

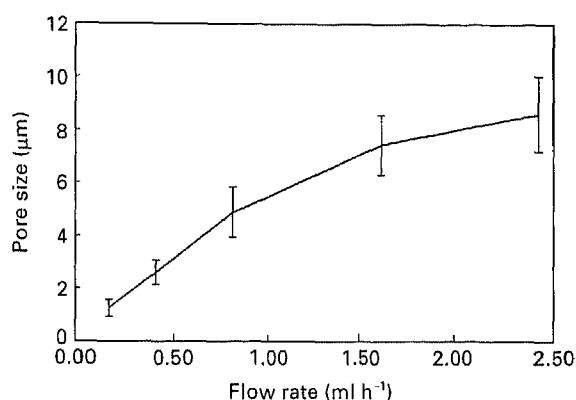


Figure 3 Relation between the pore size of  $\text{LiCoO}_2$  layers deposited at 230 °C and the flow rate of the precursor solution.

assumed that no droplet disruption occurs during droplet flight. Furthermore, we assume that one primary droplet forms a ring-like pore on the substrate. If the diameter of the ring (or pore size) is  $d_p$  and the cross-sectional area of the ring edge is  $S_p$ , then  $d_p = m/(\pi\rho S_p)$ , where  $\rho$  is the density of the deposit (here  $\text{LiCoO}_2$ ). If  $S_p$  does not change with the flow rate  $Q$ , then the pore size,  $d_p$ , is proportional to the flow rate,  $Q$ . This is roughly the case in Fig. 2a–c. However, the pore walls become considerably thicker at higher  $Q$  values as shown in Fig. 2d. At still higher  $Q$  values the pore walls become still thicker in addition to a more three-dimensionally cross-linked structure (Fig. 2e). Their pore sizes,  $d_p$ , deviate from the proportionality relation by both factors. Note, with the low limit flow rate of our pump, the pore size in Fig. 2a is very close to 1 μm. Nevertheless, according to the above model, the pore size may be reduced to the sub-micrometre range with a smaller flow rate.

Heat treatment of these layers at a temperature higher than 230 °C caused minor weight losses, prob-

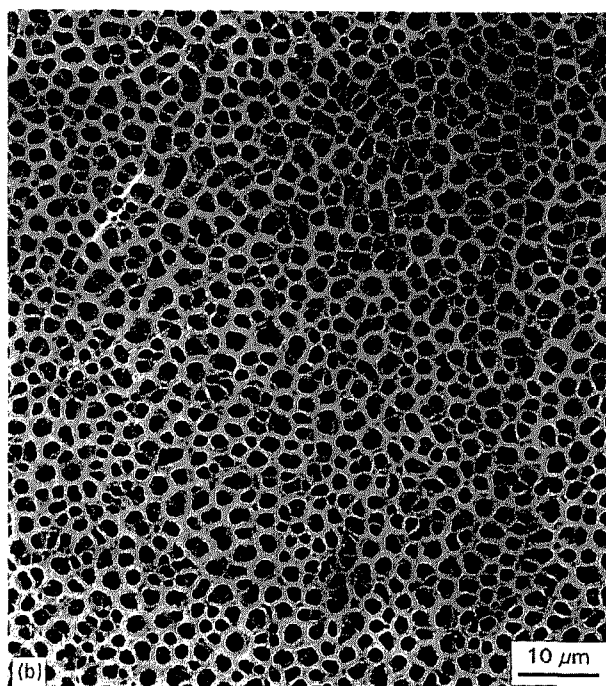
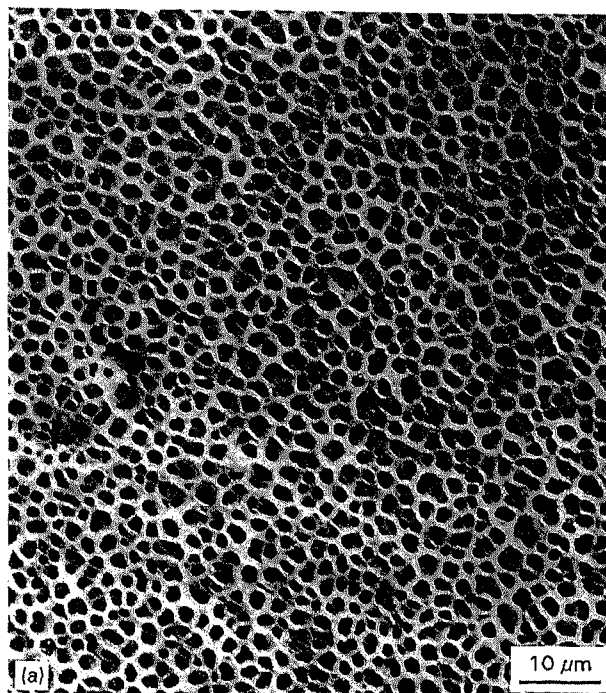


Figure 4 Scanning electron micrographs of the layer in Fig. 2b after heat treatment at two higher temperatures for 2 h with heating/cooling rate of 60 °C h<sup>-1</sup>. (a) 350 °C; (b) 600 °C.

ably due to the removal of some organic components. However, the basic porous structures remained intact after the treatment, as shown in Fig. 4. It is known that at these temperatures (350 and 600 °C)  $\text{LiCoO}_2$  with a rock salt structure must be formed [3]. A careful comparison indicates that the pore walls become slightly thicker and thus pore sizes slightly decrease after the high-temperature treatment. This might be attributed to reaction and sintering effects.

Fig. 5 shows the surface morphologies of layers deposited at two higher temperatures. It can be seen that the morphology changes considerably. Although the layer deposited at 270 °C still shows a porous

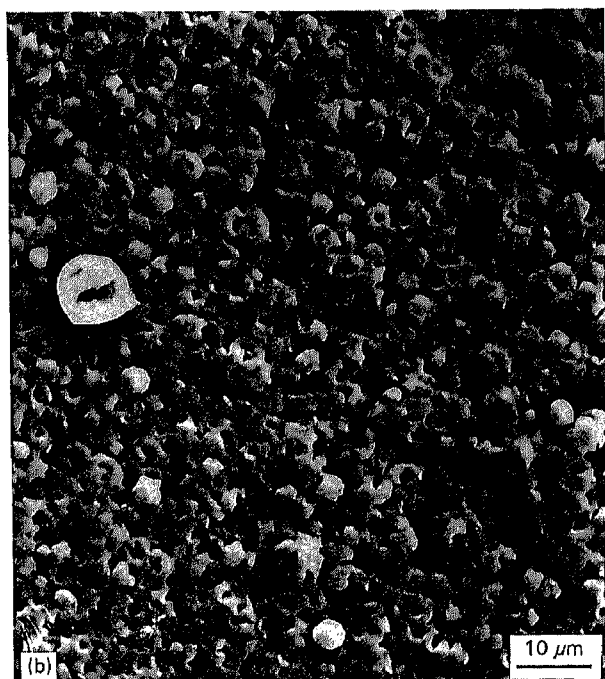
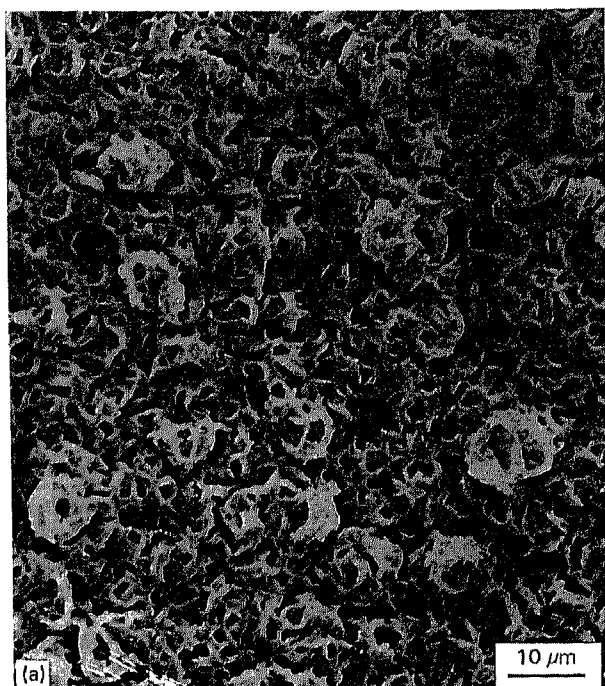


Figure 5 Scanning electron micrographs of  $\text{LiCoO}_2$  layers deposited in 2 h at (a)  $270^\circ\text{C}$  and (b)  $300^\circ\text{C}$ . The flow rate was  $1.616 \text{ ml h}^{-1}$ .

structure, the porosity markedly decreases and the shape of the pore walls is no longer regular. At  $300^\circ\text{C}$  the porosity further decreases, and the layer consists of many small thick-walled “rings” which are packed randomly. The average diameter of these “rings” (about  $2.5 \mu\text{m}$ ) is smaller than that deposited at  $230^\circ\text{C}$  with the same flow rate (Fig. 2d). Fig. 6 shows that such porous structure can also be obtained with a horizontal set-up [3], where the substrate is placed vertically except that the pore-size distribution is not as narrow as that obtained with a vertical set-up. This suggests that the gravitational force does not play a critical role in the formation of such structure. In

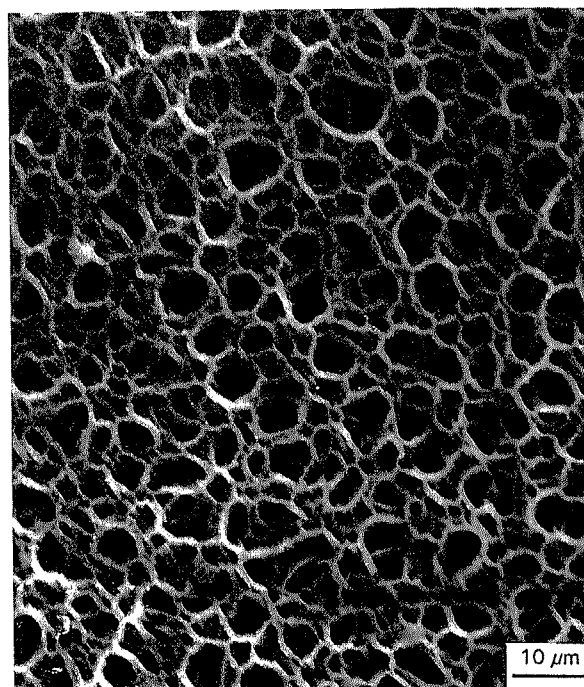


Figure 6 Scanning electron micrograph of a  $\text{LiCoO}_2$  layer deposited on stainless steel in 2 h at  $230^\circ\text{C}$  in a horizontal ESD set-up. The flow rate was  $1.616 \text{ ml h}^{-1}$ .

addition, changing the polarity of the high voltage (a negative high voltage is applied to the nozzle and keeping the substrate still grounded) the same porous layers are also obtained, which indicates that the charge sign of the charged droplets hardly affects the deposition process.

### 3.1. The model

Based on the above results and observations, we propose a possible formation scheme for such a porous structure as illustrated in Fig. 7. As mentioned before, it is assumed that there is no droplet disruption during flight. Also, the evaporation of the solvent from the droplets is far from complete before reaching the substrate surface (Fig. 7a). Therefore, when the droplets reach the substrate surface they are still wet (Fig. 7b). The impact of these solution droplets at the substrate surface leads to the spreading of the solution or wetting of the substrate (Fig. 7c). Simultaneously, the heat transfer from the substrate to the solution results in evaporation of the solvent. Because the local temperature at the edge part of a landed droplet is higher than the temperature in the middle part, the solvent evaporation proceeds faster and leads to an inhomogeneous concentration profile in the solution (Fig. 7d). With the evaporation occurring, the nucleation and precipitation of the solute take place first at the edge part. Then the precipitates become seeds where further precipitation preferably take place. Therefore, the solution in the middle part tends to flow towards the edge part. Further evaporation of the solvent at the edge part may form “rings” of the concentrated solution. This is similar to the formation of “crust” particles during powder production by means of spray pyrolysis techniques, for instance, the

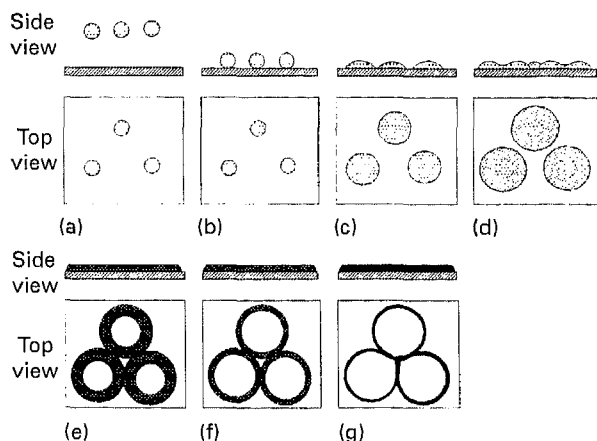


Figure 7 A formation scheme of the porous structure.

synthesis of  $\text{SnO}_2$  powder by ESP [7]. If the substrate temperature is not very high, these "rings" may be in contact with each other (Fig. 7e). Further evaporation causes the shrinkage of the ring thickness (Fig. 7f). Finally, the solvent is evaporated completely and an interconnected porous structure is formed (Fig. 7g). Because the landing of solution droplets is a continuous process, the layer will finally be three-dimensionally cross-linked. In addition, it is assumed that during the deposition process, droplet solution will not penetrate through the earlier formed porous structure. This is only possible when the interfacial surface tension between the solution and the earlier deposited layer meets a certain requirement. Note, the decomposition and reaction of the solute(s) may take place at any step, i.e. from (d) to (g) in Fig. 7, depending on the substrate temperature and the temperatures necessary for decomposition and reaction.

Basically, the above proposed mechanism may be regarded as a physical model. Based on this mechanism, it can be understood that the most important factors to influence the formation of porous structures include the substrate temperature, the boiling point of the solvent, and the spreading behaviour of the solution, that is, its surface tension and viscosity. When the substrate temperature is too high, the evaporation is so fast that spreading of the solution cannot reach the point where solution spreading edges from neighbouring droplets are in contact with each other. Thus, many separate "rings" are formed in the layer. This is the case in Fig. 5b. A somewhat lower temperature may lead to contacting "rings", but the shrinkage of the ring thickness is relatively slow, so that the pore walls are thicker than at a further lower temperature, as shown in Fig. 5a. However, there might also be some chemical driving forces resulting in the formation of this structure, because we have not obtained this structure by using nitrates instead of acetates as precursors. The chemical driving force enters, for instance, in the decomposition and reaction temperature.

Fig. 8 shows a  $\text{LiCoO}_2$  layer deposited on a porous nickel substrate. It is also porous, although it is not a continuous layer, probably due to the broad pore-size distribution and the large roughness of the nickel

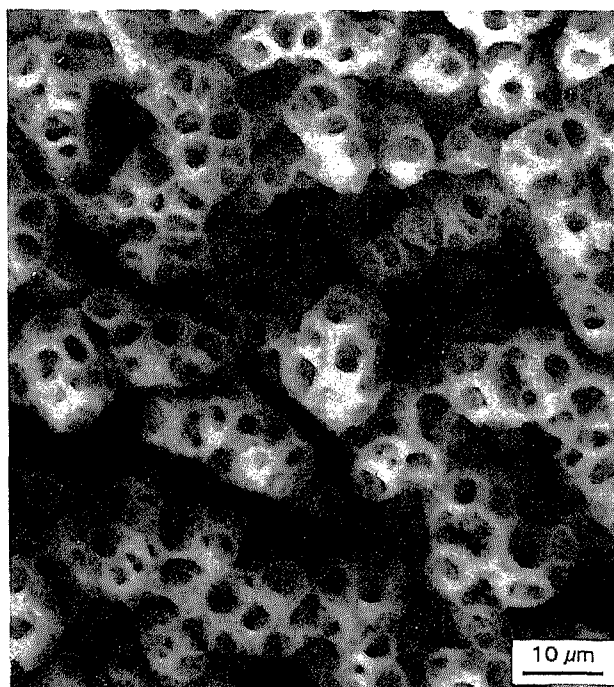


Figure 8 Scanning electron micrograph of a  $\text{LiCoO}_2$  layer deposited in 2 h on a porous nickel substrate at  $230^\circ\text{C}$ . The flow rate was  $0.808\text{ ml h}^{-1}$ .

substrate. The pore walls are thicker than those on a dense substrate, as shown in previous figures. Nonetheless, the three-dimensionally interconnected porous structure is more obvious.

#### 4. Conclusions

1. With  $\text{Li}(\text{CH}_3\text{COO})\cdot 2\text{H}_2\text{O}$  and  $\text{Co}(\text{CH}_3\text{COO})_2\cdot 4\text{H}_2\text{O}$  as precursors, 85 vol % butyl carbitol–15 vol % ethanol as the solvent, unique porous layers of  $\text{LiCoO}_2$  on some metal substrate have been prepared at  $230^\circ\text{C}$  by means of the ESD technique. The structure is thermally stable at elevated temperatures.

2. The pore size of such a layer increases with increasing flow rate of the precursor solution. At small flow rates, a nearly linear relation is found between the two parameters.

3. With increasing substrate temperature, the porosity decreases considerably, the pore walls become thicker, and the pore-size distribution becomes broader with respect to the deposition at  $230^\circ\text{C}$ .

4. A possible formation mechanism is proposed based on the present results. The substrate temperature, the boiling point of the solvent, and the surface tension of the solution are thought to be the most important factors affecting the morphology.

#### Acknowledgements

The Foundation for Chemical Research in the Netherlands (SON) under the Dutch Organization for Scientific Research (NWO) is acknowledged for the financial support. The authors are also grateful to A. A. J. Buysman for his experimental assistance.

## References

1. A. A. VAN ZOMEREN, E. M. KELDER, J. C. M. MARIJNISSEN and J. SCHOONMAN, *J. Aerosol Sci.* **25** (1994) 1229.
2. E. M. KELDER, O. C. J. NIJS and J. SCHOONMAN, *Solid State Ionics* **68** (1994) 5.
3. C. H. CHEN, A. J. J. BUYSMAN, E. M. KELDER and J. SCHOONMAN, *ibid.* **80** (1995) 1.
4. C. H. CHEN, E. M. KELDER, P. J. J. M. VANDER PUT and J. SCHOONMAN, *J. Mater. Chem.*, accepted.
5. A. J. J. BUYSMAN, C. H. CHEN, E. M. KELDER and J. SCHOONMAN, to be submitted.
6. J. ROSELL-LIOMPART and J. F. DE LA MORA, *J. Aerosol Sci.* **25** (1994) 1093.
7. P. H. W. VERCOULEN, D. M. A. CAMELOT, J. C. M. MARIJNISSEN, S. PRATSINIS and B. SCARLETT, in "Proceeding of International Workshop on the Synthesis and Measurements of Ultrafine Particles", May 1993, edited by J. C. M. Marijnissen and S. Pratsinis (Delft University Press, Delft, 1993) p. 71.

*Received 30 August  
and accepted 7 November 1995*